

Boltzmann machine learning with a variational quantum algorithm

Yuta Shingu,^{1,2} Yuya Seki,² Shohei Watabe,¹ Suguru Endo,^{3,4} Yuichiro Matsuzaki,² Shiro Kawabata,² Tetsuro Nikuni,¹ and Hideaki Hakoshima²

¹*Department of Physics, Faculty of Science Division I,
Tokyo University of Science, Shinjuku, Tokyo 162-8601, Japan.*

²*Device Technology Research Institute, National Institute of Advanced Industrial Science and Technology (AIST),
1-1-1 Umezono, Tsukuba, Ibaraki 305-8568, Japan.*

³*Department of Materials, University of Oxford, Parks Road, Oxford OX1 3PH, United Kingdom*

⁴*NTT Secure Platform Laboratories, NTT Corporation, Musashino 180-8585, Japan.*

Boltzmann machine is a powerful tool for modeling probability distributions that govern the training data. A thermal equilibrium state is typically used for Boltzmann machine learning to obtain a suitable probability distribution. The Boltzmann machine learning consists of calculating the gradient of the loss function given in terms of the thermal average, which is the most time consuming procedure. Here, we propose a method to implement the Boltzmann machine learning by using Noisy Intermediate-Scale Quantum (NISQ) devices. We prepare an initial pure state that contains all possible computational basis states with the same amplitude, and apply a variational imaginary time simulation. Readout of the state after the evolution in the computational basis approximates the probability distribution of the thermal equilibrium state that is used for the Boltzmann machine learning. We actually perform the numerical simulations of our scheme and confirm that the Boltzmann machine learning works well by our scheme.

I. INTRODUCTION

Boltzmann machine (BM) [1, 2] is a parametric stochastic model for the statistical machine learning. In the statistical machine learning, constructing a suitable generative model for given data set is an important task. It is proven that restricted Boltzmann machine (RBM) [3–5], which is a variant of BM, can approximate any discrete distribution [6], and hence RBM is a versatile model to represent an unknown distribution behind the given data set. RBM has already been used in many applications such as dimensionality reduction [7], collaborative filtering [8], classification [9], topic modelling [10], feature learning [11], and deep learning [12–15]. All the aforesaid applications adopt approximate methods for learning process of BM because the process of the original BM requires calculations of expectation values with respect to the Boltzmann distribution of the model describing the thermal equilibrium state, which are in general computationally hard. To mitigate the computational cost, many approximate algorithms on classical computers have been used [16–22]. As such, developing efficient algorithms to calculate the expectation values is attracting the interest of researchers in the field of machine learning.

In order to enhance the performance of machine learning tasks, quantum machine learning, that is machine learning by using quantum computers, has been proposed. There are many algorithms of quantum machine learning with fault-tolerant quantum computers, such as quantum support vector machine [23], linear regression [24], data fitting [25], and quantum principal component analysis [26]. Meanwhile, great efforts have been devoted to develop quantum algorithms and hardware in the near term intermediate scale quantum (NISQ) era [27]. Variational quantum algorithms (VQAs) have been considered

to be the first useful application on NISQ computers, because they only need shallow quantum circuits [28–32]. In VQAs, trial wave functions are generated from parametrized shallow depth quantum circuits and parameters are optimised by classical computers. Considering parametrised quantum circuits as a quantum analogue of a classical neural network, one may be able to implement machine learning tasks, e.g., quantum circuit learning for supervised learning [33] and data-driven quantum circuit learning for generative modelling [34]. As quantum circuits are used for generating the trial wave function, one can leverage exponentially increasing Hilbert space in the number of qubits, which may enhance the representability of the model significantly.

Motivated by the recent development of the quantum machine learning with NISQ device, we propose a new scheme to implement the BM learning by using NISQ device based on the variational imaginary time simulation. A Gibbs state can be prepared by leveraging thermofield-double technique combined with the variational imaginary time simulation [31], and we can in principle use this state for Boltzmann machine learning. However, this technique needs two copies of quantum states, which is not necessarily ideal for NISQ devices because the number of qubits is quite restricted for them. Instead, in order to reduce the number of the required qubits, we use a pure initial state that contains all possible computational basis states with the same amplitude (that is a separable state of $|+\dots+\rangle$ where $|+\rangle = \frac{1}{\sqrt{2}}(|0\rangle + |1\rangle)$ is an eigenstate of $\hat{\sigma}_x$), and perform the imaginary time evolution on the initial state to obtain the desired state. By reading out the state in the computational basis after applying the variational imaginary time simulation algorithm, the probability distribution becomes the same as what is required for the BM learning. Importantly, the necessary number of the qubits of our scheme is halved

compared to the previous approach to prepare the Gibbs state [31]. As the number of qubits is limited in NISQ devices, our efficient scheme to use fewer qubits would have a practical advantage.

The rest of this paper is organized as follows. In section II, we explain the standard setup of BM learning. In section III, we give the outline of the variational imaginary time simulation. In section IV, we propose our algorithm of BM learning with the variational imaginary time simulation. In section V, we show the numerical results of our algorithm. In section VI, we compare our method with other schemes of BM learning. Finally, we conclude and summarize this paper, in section VII.

II. BOLTZMANN MACHINE LEARNING

Boltzmann machine is a generative model that generates binary data according to a certain probability distribution. Let $\boldsymbol{\sigma} \in \{-1, 1\}^N$ be a set of binary parameters where σ_i denotes i -th component and N is the total number of the unit. First, we define the learning model $P(\boldsymbol{\sigma}|\mathbf{u})$ of BM by

$$P(\boldsymbol{\sigma}|\mathbf{u}) = \frac{1}{Z(\mathbf{u})} \exp[-H(\boldsymbol{\sigma}, \mathbf{u})], \quad (1)$$

$$H(\boldsymbol{\sigma}, \mathbf{u}) = -\sum_{i < j} J_{ij} \sigma_i \sigma_j - \sum_{i=1}^N h_i \sigma_i, \quad (2)$$

where $H(\boldsymbol{\sigma}, \mathbf{u})$ denotes the Ising Hamiltonian, $P(\boldsymbol{\sigma}|\mathbf{u})$ denotes the Boltzmann distribution, $Z(\mathbf{u})$ the partition function, and \mathbf{u} a vector of the parameters of the Hamiltonian $\mathbf{u} = (J_{12}, J_{13}, \dots, J_{N-1N}, h_1, \dots, h_N)^T$. A lower energy (the value of $H(\boldsymbol{\sigma}, \mathbf{u})$) configuration of $\boldsymbol{\sigma}$ has a larger probability $P(\boldsymbol{\sigma}|\mathbf{u})$ based on Eq. (1).

We define an empirical distribution $P_D(\boldsymbol{\sigma})$ derived from a training data-set as follows.

$$P_D(\boldsymbol{\sigma}) = \frac{1}{D} \sum_{d=1}^D \delta(\boldsymbol{\sigma}, \boldsymbol{\sigma}^{(d)}), \quad (3)$$

where $\delta(\mathbf{x}, \mathbf{y})$ denotes a Kronecker delta of N dimensions, D denotes the total number of the training data, and $\boldsymbol{\sigma}^{(d)} \in \{-1, 1\}^N$ ($d = 1, \dots, D$) denotes d th binary values of the training data.

Our aim is to find optimal parameters \mathbf{u} such that the distribution in Eq (3) can be well reproduced by $P(\boldsymbol{\sigma}|\mathbf{u})$. For this purpose, we need to adopt a measure to quantify a distance between two probability distributions, and we minimize the distance between them by choosing the optimized parameters. Specifically, we adopt the Kullback-Leibler divergence (KLD) as a measure:

$$\text{KL}(P_D||P) = \sum_{\boldsymbol{\sigma} \in \{-1, 1\}^N} P_D(\boldsymbol{\sigma}) \log \frac{P_D(\boldsymbol{\sigma})}{P(\boldsymbol{\sigma}|\mathbf{u})}. \quad (4)$$

The KLD is always greater than or equal to zero ($\text{KL}(P_D||P) \geq 0$), and the KLD becomes zero if and only if two probability distributions are identical. Minimization of the KLD over the parameter \mathbf{u} is equivalent to the maximum likelihood estimation as a function of \mathbf{u} . We use the gradient method to minimize the KLD over \mathbf{u} at the s -th update

$$\mathbf{u}[s+1] = \mathbf{u}[s] - \eta \left[\frac{\partial}{\partial \mathbf{u}} \text{KL}(P_D||P) \right] \Big|_{\mathbf{u}=\mathbf{u}[s]}, \quad (5)$$

where η denotes a learning rate satisfying $0 < \eta \ll 1$, $\mathbf{u}[s] = (J_{12}[s], \dots, J_{N-1N}[s], h_1[s], \dots, h_N[s])^T$ denotes the set of the learning parameter at the s -th update, and $\partial/\partial \mathbf{u} = (\partial/\partial J_{12}, \dots, \partial/\partial J_{N-1N}, \partial/\partial h_1, \dots, \partial/\partial h_N)^T$ denotes the nabla operator of the parameter \mathbf{u} . By rewriting the derivative in Eq. (5), we obtain the following expression:

$$\frac{\partial \text{KL}(P_D||P)}{\partial \mathbf{u}} = - \left\langle \frac{\partial H(\boldsymbol{\sigma}, \mathbf{u})}{\partial \mathbf{u}} \right\rangle + \frac{1}{D} \sum_{d=1}^D \frac{\partial H(\boldsymbol{\sigma} = \boldsymbol{\sigma}^{(d)}, \mathbf{u})}{\partial \mathbf{u}}, \quad (6)$$

where $\langle f(\boldsymbol{\sigma}) \rangle = \sum_{\boldsymbol{\sigma}} f(\boldsymbol{\sigma}) P(\boldsymbol{\sigma}|\mathbf{u})$ denotes an expectation value associated with $P(\boldsymbol{\sigma}|\mathbf{u})$, which corresponds to a thermal equilibrium average of $f(\boldsymbol{\sigma})$. In Eq. (6), the first term is the expectation value and the second term is the average with respect to training data. The second term does not depend on \mathbf{u} , and so we should calculate only the first term every time we update the parameters \mathbf{u} . However, a brute force approach to calculate the first term needs $\mathcal{O}(2^N)$ step, which is not tractable. In this paper, we propose a method to use a quantum algorithm to calculate the thermal equilibrium average.

III. VARIATIONAL IMAGINARY TIME SIMULATION

We here review the variational imaginary time simulation, which is compatible with NISQ devices. The Wick-rotated Schrödinger equation describing the imaginary time evolution can be written as [31, 35]:

$$\frac{d|\psi(\tau)\rangle}{d\tau} = -(\hat{H} - \langle \psi(\tau) | \hat{H} | \psi(\tau) \rangle) |\psi(\tau)\rangle. \quad (7)$$

The state at time τ is expressed as:

$$|\psi(\tau)\rangle = \frac{\exp(-\hat{H}\tau) |\psi(0)\rangle}{\sqrt{\langle \psi(0) | \exp(-2\hat{H}\tau) | \psi(0) \rangle}}, \quad (8)$$

whose norm is unity.

In the variational imaginary time simulation algorithm introduced in Ref. [35], instead of directly simulating

Eq. (7), one employs the parametrized wave function $|\varphi(\vec{\theta}(\tau))\rangle$ on a parametrized quantum circuit:

$$\begin{aligned} |\varphi(\vec{\theta}(\tau))\rangle &= U(\vec{\theta})|\bar{0}\rangle \\ U(\vec{\theta}) &:= U_N(\theta_N)\dots U_k(\theta_k)\dots U(\theta_1), \end{aligned} \quad (9)$$

where $U_k(\theta_k)$ corresponds to a parametrized gate constituting the variational quantum circuit, θ_k is a real parameter and $|\bar{0}\rangle$ is an initial state of this ansatz which is usually chosen to be equal to $|\psi(0)\rangle$.

Then, Eq. (7) is mapped onto the evolution of the parameters. Here, we use the McLachlan variational principle [36, 37] to derive the time derivative equations for $\vec{\theta}(\tau)$. Following the principle, we minimize the distance between the exact evolution and that of the parametrized trial state as

$$\delta \left\| \left(\frac{\partial}{\partial \tau} + \hat{H} - \langle \varphi(\vec{\theta}(\tau)) | \hat{H} | \varphi(\vec{\theta}(\tau)) \rangle \right) |\varphi(\vec{\theta}(\tau))\rangle \right\| = 0, \quad (10)$$

which leads to

$$M \frac{\partial \vec{\theta}(\tau)}{\partial \tau} = \vec{C}, \quad (11)$$

where

$$M_{k,j} = \Re \left(\frac{\partial \langle \varphi(\vec{\theta}(\tau)) |}{\partial \theta_k} \frac{\partial |\varphi(\vec{\theta}(\tau))\rangle}{\partial \theta_j} \right), \quad (12)$$

$$C_k = -\Re \left(\langle \varphi(\vec{\theta}(\tau)) | \hat{H} \frac{\partial |\varphi(\vec{\theta}(\tau))\rangle}{\partial \theta_k} \right). \quad (13)$$

Here, $\| |\varphi\rangle \| = \langle \varphi | \varphi \rangle$. Solving Eq. (11), for a small interval $\delta\tau$, the imaginary time evolution can be approximately simulated when we use a suitable update rule

$$\vec{\theta}(\tau + \delta\tau) \simeq \vec{\theta}(\tau) + M^{-1}(\tau) \cdot C(\tau) \delta\tau, \quad (14)$$

where we use the Euler method.

Note that each element of M and \vec{C} can be evaluated on quantum circuits efficiently. The derivative of parametrized gates can generally be represented as:

$$\frac{\partial U_k}{\partial \theta_k} = \sum_i a_{k,i} U_k \hat{u}_{k,i}. \quad (15)$$

Here, $\hat{u}_{k,i}$ is a unitary operator, with $a_{k,i}$ being a complex coefficient. For example, $dU_k/d\theta_k = -i\hat{\sigma}_x U_k(\theta_k)$, and one can see $a_{k,i} = -i$ and $u_{k,i} = \hat{\sigma}_x$. Thus, the derivative of the parametrized state $|\varphi(\vec{\theta}(\tau))\rangle$ is

$$\frac{\partial |\varphi(\vec{\theta}(\tau))\rangle}{\partial \theta_k} = \sum_i a_{k,i} U_{k,i} |\bar{0}\rangle, \quad (16)$$

where

$$U_{k,i} = U_N \cdots U_{k+1} U_k \hat{u}_{k,i} U_{k-1} \cdots U_1. \quad (17)$$

Using Eq. (17), one can express $M_{k,j}$ as

$$M_{k,j} = \sum_{p,q} \Re \left(a_{k,p}^* a_{j,q} \langle \bar{0} | U_{k,p}^\dagger U_{j,q} |\bar{0}\rangle \right). \quad (18)$$

For \vec{C} , assuming that the Hamiltonian \hat{H} can be decomposed as $\hat{H} = \sum_j f_j \hat{P}_j$, where f_j is real and \hat{P}_j is a tensor product of Pauli operators, we obtain

$$C_k = - \sum_{i,j} \Re \left(a_{k,i} f_j \langle \bar{0} | U^\dagger(\vec{\theta}) \hat{P}_j U_{k,i} |\bar{0}\rangle \right), \quad (19)$$

Notice that all the elements of M and \vec{C} can be represented in the form of

$$b \Re (e^{i\phi} \langle \bar{0} | V |\bar{0}\rangle),$$

where b and ϕ are real parameters determined by $a_{k,i}$, and V is a unitary operator, which is either $U_{k,p}^\dagger U_{j,q}$ or $U^\dagger \hat{P}_j U_{k,i}$. One can compute elements of M and \vec{C} by leveraging quantum circuits shown in Fig. 1.

IV. BM LEARNING WITH VARIATIONAL IMAGINARY TIME SIMULATION

In this section, we describe our proposal of a quantum algorithm to calculate the thermal equilibrium average in Eq. (6). Especially, we adopt the variational imaginary time simulation described in the previous section. For this purpose, we replace σ_i in the Hamiltonian (2) with the Pauli matrix $\hat{\sigma}_{z,i}$. We define the eigenstates of $\hat{\sigma}_z$ by $|0\rangle, |1\rangle$ ($\hat{\sigma}_z |0\rangle = |0\rangle, \hat{\sigma}_z |1\rangle = -|1\rangle$).

We thus introduce the quantum Hamiltonian as follows.

$$\hat{H}(\mathbf{u}) = - \sum_{i<j} J_{ij} \hat{\sigma}_{z,i} \hat{\sigma}_{z,j} - \sum_{i=1}^N h_i \hat{\sigma}_{z,i} \quad (20)$$

By using the variational imaginary time simulation, we can prepare such as

$$|\psi_{\mathbf{u}}\rangle = \sqrt{\frac{2^N}{Z(\mathbf{u})}} e^{-\hat{H}(\mathbf{u})/2} |++\cdots+\rangle, \quad (21)$$

using the initial state $|++\cdots+\rangle$. Here, $|+\rangle = (|0\rangle + |1\rangle)/\sqrt{2}$ and $|++\cdots+\rangle = |+\rangle \otimes |+\rangle \otimes \cdots \otimes |+\rangle$.

Once Eq. (21) is prepared, one can calculate the thermal equilibrium average in the right hand side of Eq. (6) as follows:

$$\left\langle \frac{\partial H(\boldsymbol{\sigma}, \mathbf{u})}{\partial \mathbf{u}} \right\rangle = \left\langle \psi_{\mathbf{u}} \left| \frac{\partial \hat{H}(\mathbf{u})}{\partial \mathbf{u}} \right| \psi_{\mathbf{u}} \right\rangle. \quad (22)$$

This is because $|\psi_{\mathbf{u}}\rangle = \sum_{\boldsymbol{\sigma}} \sqrt{P(\boldsymbol{\sigma}|\mathbf{u})} |\boldsymbol{\sigma}\rangle$ and the density operator corresponding to $|\psi_{\mathbf{u}}\rangle$ has all the same diagonal elements about the computational basis as those of

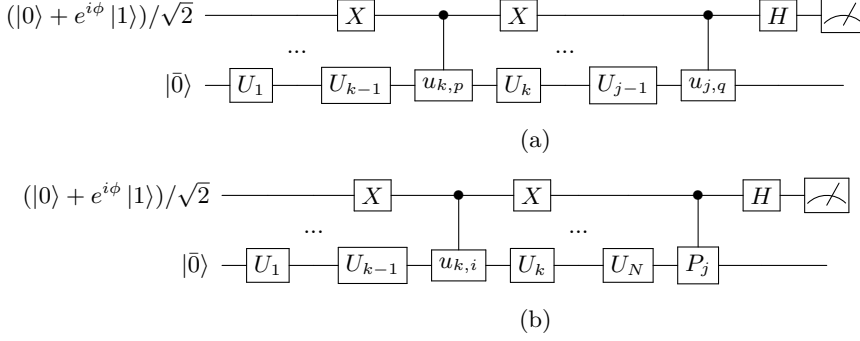


FIG. 1. Quantum circuits for calculating (a) $\Re(e^{i\phi} \langle \bar{0} | U_{k,p}^\dagger U_{j,q} | \bar{0} \rangle)$ and (b) $\Re(e^{i\phi} \langle \bar{0} | U_{k,i}^\dagger \hat{P}_j U | \bar{0} \rangle)$.

the Gibbs state $e^{-\hat{H}(\mathbf{u})}/Z(\mathbf{u})$, and $\partial\hat{H}(\mathbf{u})/\partial\mathbf{u}$ has only $\hat{\sigma}_z$ terms. Note that both Eq. (8) and Eq. (21) are normalized, and therefore when the initial state $|\psi(0)\rangle = |+\dots+\rangle$ evolves from $\tau = 0$ to $\tau = 1/2$ following Eq. (7), two states are equal. This evolution is required for every update of the parameter \mathbf{u} in the learning process.

Algorithm 1 Optimization of learning parameter

Initialize \mathbf{u} with the normal distribution

for $s = 1, 2, \dots, N_{\text{step}}$ **do**

$\tau \leftarrow 0$

$\vec{\theta} \leftarrow \vec{0}$

repeat

 Calculate matrix M using Eq. (18)

 Calculate vector \vec{C} using Eq. (19)

$\vec{\theta} \leftarrow \vec{\theta} + M^{-1}\vec{C}\delta\tau$

$\tau \leftarrow \tau + \delta\tau$

until $\tau = 1/2$

$|\psi\mathbf{u}\rangle \leftarrow |\varphi(\vec{\theta})\rangle$ using Eq. (9)

$\frac{\partial\text{KL}}{\partial\mathbf{u}} \leftarrow - \left\langle \psi\mathbf{u} \left| \frac{\partial\hat{H}(\mathbf{u}')}{\partial\mathbf{u}'} \right|_{\mathbf{u}'=\mathbf{u}} \right| \psi\mathbf{u} \right\rangle$

$+ \frac{1}{D} \sum_{d=1}^D \frac{\partial H(\boldsymbol{\sigma} = \boldsymbol{\sigma}^{(d)}, \mathbf{u}')}{\partial\mathbf{u}'} \Big|_{\mathbf{u}'=\mathbf{u}}$

$\mathbf{u} \leftarrow \mathbf{u} - \eta \frac{\partial\text{KL}}{\partial\mathbf{u}}$

end for

return \mathbf{u}

V. RESULTS

In this section, we show the performance of our scheme by numerical simulations. For this purpose, we need to generate a training data. First, we randomly generate a set of parameters \mathbf{u}_l^* ($l = 1, 2, \dots, L$) where L denotes the number of the parameter sets. We use a normal distribution with a mean of 0 and a variance of 1 to generate each component of \mathbf{u}_l^* . We call \mathbf{u}_l^* true parameters. Second, for a given \mathbf{u}_l^* , we generate training data $\boldsymbol{\sigma}^{(i,l)} \in \{-1, 1\}^N$ ($i = 1, \dots, D$) based on a probabilistic distribution of $P(\boldsymbol{\sigma}|\mathbf{u}_l^*)$, which provides us with L

groups of the training data. Third, we calculate $P_D^{(l)}(\boldsymbol{\sigma})$ in Eq. (3) by using each group of the training data. In our numerical simulations, we adopt a case of $N = 4$, $L = 30$, and $D = 1000$.

Our simulation method with the number of iteration steps N_{step} , a fixed step size of the imaginary time evolution $\delta\tau$, and the learning rate η ($0 < \eta \ll 1$) is summarized in Algorithm 1. Here, we choose $N_{\text{step}} = 100$ and $\delta\tau = 0.1$ in the numerical simulations

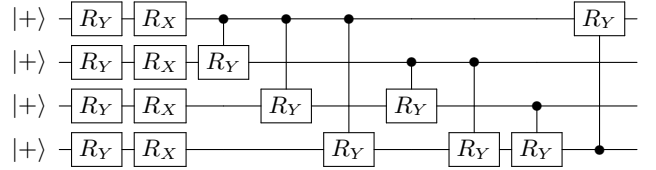


FIG. 2. Our ansatz circuit for the variational imaginary time simulation with 4 qubits.

Based on the training data, we run our algorithm as follows. First, by using one of the groups of the training data (\mathbf{u}_1^*), we perform numerical simulations of our scheme where we choose our ansatz circuit for the variational imaginary time simulation as Fig. 2, and obtain the learning parameters $\mathbf{u}_{\text{opt}}^{(l)}$ after the optimization by using the gradient method Eq. (5) from $s = 0$ to N_{step} . We need an initial guess of \mathbf{u} ($\mathbf{u}[0]$ in Eq. (5)) for the simulation, and we use the normal distribution with a mean of 0 and a variance of 1 for the initial guess at each time. Second, we can perform the same numerical simulations as the first step but by using a different group of the training data ($\mathbf{u}_2^*, \mathbf{u}_3^*, \dots, \mathbf{u}_L^*$), we obtain a different learning parameter after the optimization. We repeat this process L times. Note that, although in our numerical simulations we can directly calculate the right-hand side of the expectation value in Eq. (22), we need a sampling to obtain the expectation value when we use a quantum computer as shown in the Fig. 1.

To evaluate the performance of our scheme, we consider the KLD between the true distribution $P(\boldsymbol{\sigma}|\mathbf{u}_l^*)$

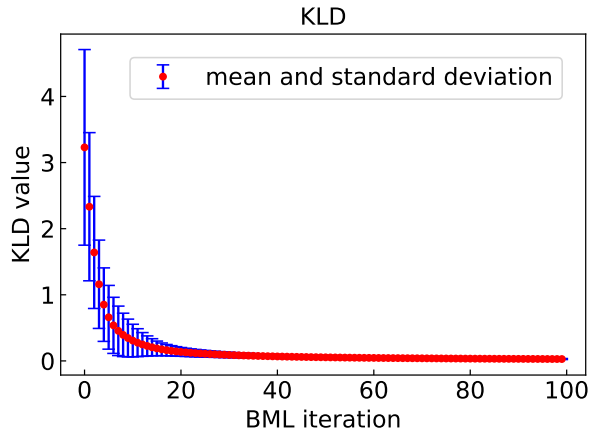


FIG. 3. The KLD between the true distribution and the obtained distribution from the imaginary time evolution at each iteration step. We take an average of KLD over all groups of training data at each step, and show each mean value and standard deviation in this plot. The KLD converges to zero, and thus our scheme based on the imaginary time evolution can reproduce the training data.

and estimated distribution $P(\sigma|\mathbf{u}^{(l)}[s])$ in Eq. (1) optimized by the variational imaginary time simulation, where $\mathbf{u}^{(l)}[s]$ denotes a learning parameter at the s -th step. Fig. 3 shows the average and standard deviation of such KLD at s -th step over the true parameters \mathbf{u}_l^* ($l = 1, 2, \dots, L$). These results show that all the average and the standard deviation of the KLD converge to zero, and thus our scheme can successfully reproduce the probability distribution that generated the training data, which shows the high performance of our proposal as BM learning.

Furthermore, we investigate how the convergence speed of the KLD depends on the given true parameters \mathbf{u}_l^* . Fig. 4 shows the histogram of the values of the KLD at 25th, 50th, and 100th iteration step, respectively. At 25th iteration step, the values of the KLD strongly depends on the true parameters \mathbf{u}_l^* . However, as we increase the iteration step, the standard deviation becomes smaller, and most of the KLD becomes close to zero at 100th iteration step.

In addition, we examine whether the variational imaginary time simulation actually provides us with the target state described in Eq. (21). It is worth mentioning that the state obtained by the variational imaginary time simulation can be different from the target state, because its performance strongly depends on the ansatz of the quantum circuit, and our machine learning algorithm may work well accidentally because we only use some parts of the expectation values in our scheme and not use the full information of the obtained state. To investigate how close the state obtained by the variational imaginary time simulation is to the target state, we plot the fidelity between them in Fig. 5. The fidelity is more than 0.995. These results show that the good agreement

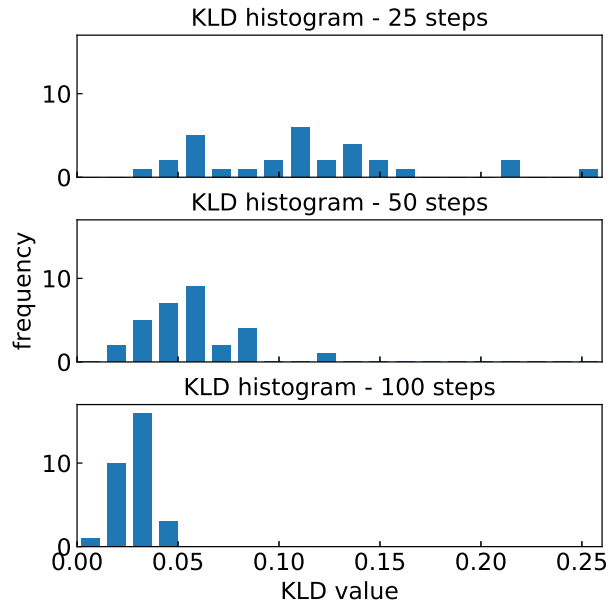


FIG. 4. The histogram of the values of the KLD at 25th, 50th, and 100th iteration steps, respectively. We set the total iteration step $N_{\text{step}} = 100$. The range of the KLD values is from 0 to 0.26, and we divide it into 20 bins. We plot the histogram as the number of the counts in each bin.

between the obtained state and target state.

VI. COMPARISON WITH OTHER SCHEMES OF BOLTZMANN MACHINE LEARNING

An interesting question for future work is whether our scheme is more useful due to the quantum properties or not, compared with the classical scheme of the BM learning such as Markov-chain Monte Carlo samplings [38]. To answer this question, we need a careful benchmark of the performance of our scheme by using an actual NISQ device, because it is difficult to obtain an analytical proof of quantum speedup as with many other NISQ algorithms. We leave this for future work. However, without such an assessment about the quantum speedup, our work presented in this paper could still contribute to the society for the following two reasons. First, most of the implementations of the BM learning are heuristic, and thus they may not always be able to find the suitable solution if we focus on just a specific implementation. Therefore it is better if we have more options to perform the BM learning for searching the suitable solutions. Second, a quantum algorithm based on gate operations is compatible with a protocol called blind quantum computation [39]. Here, a client can safely delegate a quantum algorithm to a server who has a gate-type quantum computer, and the server cannot steal any information

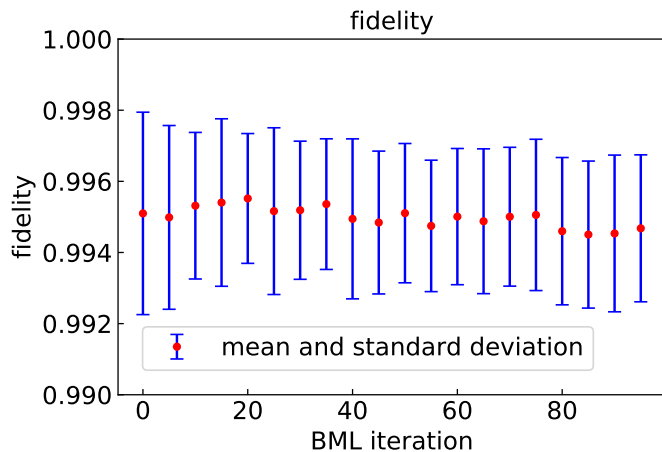


FIG. 5. The fidelity between the target state described in the Eq. (21) and the obtained state from the variational imaginary time simulation against the iteration steps. The fidelity is around or more than 0.995 at every iteration step. These results show that our ansatz circuit is suitable to generate the target state $|\psi_{\mathbf{u}}\rangle$ (21) with a reasonably good approximation.

about what the client performs with the server machine where the security is based on fundamental physics law such as no-signaling principle [40]. Therefore, in principle, our scheme can be implemented with blind quantum computation, while information-theoretically secure BM learning is not known in classical implementations.

Let us compare our scheme with other approaches for BM learning with quantum devices. First, there are works on the preparation of Eq. (21) by using quantum annealing machine. They construct the Hamiltonian whose ground state of which is equal to Eq. (21). However, such a Hamiltonian includes many-body (more than three-body) interactions and is difficult to realize experimentally. Second, with the NISQ device, there is another method to create a thermal equilibrium state by minimizing the free energy function with a fixed temperature [41–46]. Nevertheless, the free energy function is determined by the energy expectation value and the von

Neumann entropy, and it is a non-trivial problem to calculate the von Neumann entropy on a relatively shallow quantum circuit. Finally, only recently, the variational imaginary time simulation was used for quantum Boltzmann machine learning with numerical calculations and an IBM quantum device [47]. In their scheme, they can realize a thermal equilibrium with the Hamiltonian that contains not only $\hat{\sigma}_z$ terms but also $\hat{\sigma}_x$ and $\hat{\sigma}_y$ terms. A trade off is that their scheme requires to double the number of qubits with respect to the number of units in the original problem, which is twice as large as that of ours, which would show practical advantage of our scheme for implementing the BM learning by using just σ_z terms.

VII. CONCLUSION

In conclusion, we propose a scheme to implement BM learning based on the variational imaginary time simulation with NISQ devices. Unlike the previous approaches that prepare a thermal equilibrium state [31], we use a pure state whose distribution mimics the thermal equilibrium distribution. The necessary number of the qubits of our scheme is twice smaller than that of the previous scheme to use the imaginary time evolution to prepare the Gibbs state [31]. Our results show potential for an efficient use of the NISQ device for the BM learning.

ACKNOWLEDGMENTS

We thank Dr. Muneki Yasuda for useful comments on BM. This work was supported by Leading Initiative for Excellent Young Researchers MEXT Japan and JST presto (Grant No. JPMJPR1919) Japan. This work was partly supported by MEXT Q-LEAP (JPMXS0118068682), and JST ERATO (JPMJER1601). S.W. was supported by Nanotech CUPAL, National Institute of Advanced Industrial Science and Technology (AIST).

While this manuscript was being written, an independent article [47] that proposed quantum Boltzmann machine [48], which prepares a Gibbs state by leveraging thermofield-double technique combined with the variational imaginary time simulation [31].

-
- [1] Scott E Fahlman, Geoffrey E Hinton, and Terrence J Sejnowski. Massively parallel architectures for al: Netl, thistle, and boltzmann machines. In *National Conference on Artificial Intelligence, AAAI*, 1983.
 - [2] David H Ackley, Geoffrey E Hinton, and Terrence J Sejnowski. A learning algorithm for boltzmann machines. *Cognitive science*, 9(1):147–169, 1985.
 - [3] Paul Smolensky. Information processing in dynamical systems: Foundations of harmony theory. Technical report, Colorado Univ at Boulder Dept of Computer Science, 1986.
 - [4] Vinod Nair and Geoffrey E Hinton. Rectified linear units improve restricted boltzmann machines. In *Proceedings of the 27th international conference on machine learning (ICML-10)*, pages 807–814, 2010.
 - [5] Geoffrey E Hinton. A practical guide to training restricted boltzmann machines. In *Neural networks: Tricks of the trade*, pages 599–619. Springer, 2012.
 - [6] Nicolas Le Roux and Yoshua Bengio. Representational power of restricted boltzmann machines and deep belief networks. *Neural computation*, 20(6):1631–1649, 2008.
 - [7] Geoffrey E Hinton and Ruslan R Salakhutdinov. Reducing the dimensionality of data with neural networks.

- science*, 313(5786):504–507, 2006.
- [8] Ruslan Salakhutdinov, Andriy Mnih, and Geoffrey Hinton. Restricted boltzmann machines for collaborative filtering. In *Proceedings of the 24th international conference on Machine learning*, pages 791–798, 2007.
 - [9] Hugo Larochelle and Yoshua Bengio. Classification using discriminative restricted boltzmann machines. In *Proceedings of the 25th international conference on Machine learning*, pages 536–543, 2008.
 - [10] Geoffrey E Hinton and Russ R Salakhutdinov. Replicated softmax: an undirected topic model. In *Advances in neural information processing systems*, pages 1607–1614, 2009.
 - [11] Adam Coates, Andrew Ng, and Honglak Lee. An analysis of single-layer networks in unsupervised feature learning. In *Proceedings of the fourteenth international conference on artificial intelligence and statistics*, pages 215–223, 2011.
 - [12] George E Dahl, Dong Yu, Li Deng, and Alex Acero. Context-dependent pre-trained deep neural networks for large-vocabulary speech recognition. *IEEE Transactions on audio, speech, and language processing*, 20(1):30–42, 2011.
 - [13] Geoffrey E Hinton, Simon Osindero, and Yee-Whye Teh. A fast learning algorithm for deep belief nets. *Neural computation*, 18(7):1527–1554, 2006.
 - [14] Ruslan Salakhutdinov and Geoffrey Hinton. Deep boltzmann machines. In *Artificial intelligence and statistics*, pages 448–455, 2009.
 - [15] Ruslan Salakhutdinov and Geoffrey Hinton. An efficient learning procedure for deep boltzmann machines. *Neural computation*, 24(8):1967–2006, 2012.
 - [16] Geoffrey E Hinton. Training products of experts by minimizing contrastive divergence. *Neural computation*, 14(8):1771–1800, 2002.
 - [17] Miguel A Carreira-Perpinan and Geoffrey E Hinton. On contrastive divergence learning. In *Aistats*, volume 10, pages 33–40. Citeseer, 2005.
 - [18] Yoshua Bengio and Olivier Delalleau. Justifying and generalizing contrastive divergence. *Neural computation*, 21(6):1601–1621, 2009.
 - [19] Marylou Gabri e, Eric W Tramel, and Florent Krzakala. Training restricted boltzmann machine via the thouless-anderson-palmer free energy. In *Advances in neural information processing systems*, pages 640–648, 2015.
 - [20] Benjamin Marlin, Kevin Swersky, Bo Chen, and Nando Freitas. Inductive principles for restricted boltzmann machine learning. In *Proceedings of the Thirteenth International Conference on Artificial Intelligence and Statistics*, pages 509–516, 2010.
 - [21] Muneki Yasuda, Shun Kataoka, Yuji Waizumi, and Kazuyuki Tanaka. Composite likelihood estimation for restricted boltzmann machines. In *Proceedings of the 21st International Conference on Pattern Recognition (ICPR2012)*, pages 2234–2237. IEEE, 2012.
 - [22] Muneki Yasuda, Tetsuharu Sakurai, and Kazuyuki Tanaka. Learning algorithm in restricted boltzmann machines using kullback-leibler importance estimation procedure. *Nonlinear Theory and Its Applications, IEICE*, 2(2):153–164, 2011.
 - [23] Patrick Rebentrost, Masoud Mohseni, and Seth Lloyd. Quantum support vector machine for big data classification. *Physical review letters*, 113(13):130503, 2014.
 - [24] Maria Schuld, Ilya Sinayskiy, and Francesco Petruccione. Prediction by linear regression on a quantum computer. *Physical Review A*, 94(2):022342, 2016.
 - [25] Nathan Wiebe, Daniel Braun, and Seth Lloyd. Quantum algorithm for data fitting. *Physical review letters*, 109(5):050505, 2012.
 - [26] Seth Lloyd, Masoud Mohseni, and Patrick Rebentrost. Quantum principal component analysis. *Nature Physics*, 10(9):631–633, 2014.
 - [27] John Preskill. Quantum computing in the nisq era and beyond. *Quantum*, 2:79, 2018.
 - [28] Alberto Peruzzo, Jarrod McClean, Peter Shadbolt, Man-Hong Yung, Xiao-Qi Zhou, Peter J Love, Al an Aspuru-Guzik, and Jeremy L O’Brien. A variational eigenvalue solver on a photonic quantum processor. *Nature communications*, 5:4213, 2014.
 - [29] Ying Li and Simon C Benjamin. Efficient variational quantum simulator incorporating active error minimization. *Physical Review X*, 7(2):021050, 2017.
 - [30] Jarrod R McClean, Jonathan Romero, Ryan Babbush, and Al an Aspuru-Guzik. The theory of variational hybrid quantum-classical algorithms. *New Journal of Physics*, 18(2):023023, 2016.
 - [31] Xiao Yuan, Suguru Endo, Qi Zhao, Ying Li, and Simon C Benjamin. Theory of variational quantum simulation. *Quantum*, 3:191, 2019.
 - [32] Suguru Endo, Jinzhao Sun, Ying Li, Simon C. Benjamin, and Xiao Yuan. Variational quantum simulation of general processes. *Phys. Rev. Lett.*, 125:010501, Jun 2020.
 - [33] Kosuke Mitarai, Makoto Negoro, Masahiro Kitagawa, and Keisuke Fujii. Quantum circuit learning. *Physical Review A*, 98(3):032309, 2018.
 - [34] Marcello Benedetti, Delfina Garcia-Pintos, Oscar Perdomo, Vicente Leyton-Ortega, Yunseong Nam, and Alejandro Perdomo-Ortiz. A generative modeling approach for benchmarking and training shallow quantum circuits. *npj Quantum Information*, 5(1):1–9, 2019.
 - [35] Sam McArdle, Tyson Jones, Suguru Endo, Ying Li, Simon C Benjamin, and Xiao Yuan. Variational ansatz-based quantum simulation of imaginary time evolution. *npj Quantum Information*, 5(1):1–6, 2019.
 - [36] AD McLachlan. A variational solution of the time-dependent schrodinger equation. *Molecular Physics*, 8(1):39–44, 1964.
 - [37] J Broeckhove, L Lathouwers, E Kesteloot, and P Van Leuven. On the equivalence of time-dependent variational principles. *Chemical physics letters*, 149(5-6):547–550, 1988.
 - [38] David P Landau and Kurt Binder. *A guide to Monte Carlo simulations in statistical physics*. Cambridge university press, 2014.
 - [39] Anne Broadbent, Joseph Fitzsimons, and Elham Kashefi. Universal blind quantum computation. In *2009 50th Annual IEEE Symposium on Foundations of Computer Science*, pages 517–526. IEEE, 2009.
 - [40] Tomoyuki Morimae and Keisuke Fujii. Blind quantum computation protocol in which alice only makes measurements. *Physical Review A*, 87(5):050301, 2013.
 - [41] Jingxiang Wu and Timothy H Hsieh. Variational thermal quantum simulation via thermofield double states. *Physical Review Letters*, 123(22):220502, 2019.
 - [42] D Zhu, S Johri, NM Linke, KA Landsman, NH Nguyen, CH Alderete, AY Matsuura, TH Hsieh, and C Monroe. Variational generation of thermofield double states and

- critical ground states with a quantum computer. *arXiv preprint arXiv:1906.02699*, 2019.
- [43] Guillaume Verdon, Jacob Marks, Sasha Nanda, Stefan Leichenauer, and Jack Hidary. Quantum hamiltonian-based models and the variational quantum thermalizer algorithm. *arXiv preprint arXiv:1910.02071*, 2019.
- [44] Anirban N Chowdhury, Guang Hao Low, and Nathan Wiebe. A variational quantum algorithm for preparing quantum gibbs states. *arXiv preprint arXiv:2002.00055*, 2020.
- [45] Youle Wang, Guangxi Li, and Xin Wang. Variational quantum gibbs state preparation with a truncated taylor series. *arXiv preprint arXiv:2005.08797*, 2020.
- [46] Guillaume Verdon, Michael Broughton, and Jacob Biamonte. A quantum algorithm to train neural networks using low-depth circuits. *arXiv preprint arXiv:1712.05304*, 2017.
- [47] Christa Zoufal, Aurélien Lucchi, and Stefan Woerner. Variational quantum boltzmann machines. *arXiv preprint arXiv:2006.06004*, 2020.
- [48] Mohammad H Amin, Evgeny Andriyash, Jason Rolfe, Bohdan Kulchytskyy, and Roger Melko. Quantum boltzmann machine. *Physical Review X*, 8(2):021050, 2018.